PD-1 blockade and CD27 stimulation activate distinct transcriptional programs that synergize for CD8+ T-cell driven anti-tumor immunity

Sarah L. Buchan[1, 2], Mohannad Fallatah[1, 2], Stephen M. Thirdborough[3], Vadim Y. Taraban[1, 4], Anne Rogel[1], Lawrence J. Thomas[5], Christine A. Penfold[1], Li-Zhen He[5], Michael A. Curran[6], Tibor Keler[5], Aymen Al-Shamkhani[1].

[1]Cancer Sciences Unit, Faculty of Medicine, University of Southampton, Southampton, Hants, SO16 6YD, U.K. [2]These authors contributed equally. [3]Cancer Research UK Centre, University of Southampton, Hants, SO16 6YD, U.K. [4]Current address: School of Applied Science, London South Bank University, London, U.K. SE1 0AA. [5]Celldex Therapeutics Inc, Hampton, NJ 08827, U.S.A. [6]Department of Immunology, The University of Texas MD Anderson Cancer Center, Houston, TX 77030, U.S.A.

Running Title: Synergy between PD-1/L1 blockade and CD27 agonists

Keywords: CD27, PD-1, immunotherapy, cancer, varlilumab.

Financial support: The authors would like to thank Cancer Research UK for funding. This work was also funded by Celldex Therapeutics.

Corresponding Author: Prof A. Al-Shamkhani, Cancer Sciences Unit, Faculty of Medicine, University of Southampton, Southampton, U.K., SO16 6YD, Tel: (023) 81 206285, Fax: (023) 80 704061, Email:aymen@soton.ac.uk.

Conflict of interest statement: A.A-S receives research funding from Celldex Therapeutics Inc. S.L.B., M.F., S.M.T., V.Y.T., A.R., C.A.P and M.A.C. have no financial conflicts of interest. L.J.T, L-Z.H. and T.K. are employees of Celldex Therapeutics Inc.

Word count: 4591

Main manuscript: 6 Figs

Supplementary Files: 5 Figs, 2 Tables

Statement of translational relevance

Anti-tumor effector CD8+ T cells are often suppressed by PD-1 signaling. While blocking antibodies to PD-1 and PD-L1 have shown impressive results in multiple tumor types, only a minority of patients respond and recent findings suggest that stimulatory signals for T cell activation may be lacking in some patients. We here show that agonist antibodies targeting mouse or human CD27, a key costimulatory receptor, act synergistically with anti-PD-1/L1 to increase CD8+ T-cell proliferation, effector function and tumor clearance in wild-type and human-CD27 transgenic mice. Detailed mechanistic analysis indicates co-operative, yet also independent, influences of these antibodies on aspects of T-cell activation. Thus, our data reveal synergy between anti-PD-1/L1 and anti-CD27 for immunotherapy and provide renewed impetus for clinical evaluation of combined anti-CD27 and anti-PD-1/L1.

Abstract

Purpose: PD-1 checkpoint blockade has revolutionized the field of cancer immunotherapy, yet the frequency of responding patients is limited by inadequate T-cell priming secondary to a paucity of activatory dendritic cells (DCs). DC signals can be bypassed by CD27 agonists and we therefore investigated if the effectiveness of anti-PD-1/L1 could be improved by combining with agonist anti-CD27 monoclonal antibodies (mAb).

Experimental Design: The efficacy of PD-1/L1 blockade or agonist anti-CD27 mAb was compared with a dual-therapy approach in multiple tumor models. Global transcriptional profiling and flow-cytometry analysis were used to delineate mechanisms underpinning the observed synergy.

Results: PD-1/PD-L1 blockade and agonist anti-CD27 mAb synergize for increased CD8+ T-cell expansion and effector function, exemplified by enhanced IFN-γ, TNF-α, granzyme B and T-bet. Transcriptome analysis of CD8+ T cells revealed that combination therapy triggered a convergent program largely driven by IL-2 and Myc. However, division of labor was also apparent such that anti-PD-1/L1 activates a cytotoxicity-gene expression program whereas anti-CD27 preferentially augments proliferation. In tumor models, either dependent on endogenous CD8+ T cells or adoptive transfer of transgenic T cells, anti-CD27 mAb synergized with PD-1/L1 blockade for anti-tumor immunity. Finally, we show that a clinically-relevant anti-human CD27 mAb, varlilumab, similarly synergizes with PD-L1 blockade for protection against lymphoma in human-CD27 transgenic mice.

Conclusions: Our findings suggest that suboptimal T-cell invigoration in cancer patients undergoing treatment with PD-1 checkpoint blockers will be improved by dual PD-1 blockade and CD27 agonism and provide mechanistic insight into how these approaches co-operate for CD8+ T-cell activation.

Introduction

While it is clear that activated CD8+ T cells can be harnessed to kill tumor cells, T-cell activation is a complex, multifaceted process, tightly controlled by activatory and inhibitory receptors. To effectively utilise T cells for immunotherapy it is therefore necessary to understand how these signals can be exploited to support appropriate T-cell activation. PD-1 is a well-studied inhibitory receptor triggered by binding to PD-L1 or PD-L2, and which counters T-cell activation through a mechanism dependent on recruitment of the protein tyrosine phosphatase SHP-2 to an immunoreceptor based tyrosine switch motif (ITSM) in its cytoplasmic tail. Subsequent signaling events act to repress TCR-driven signals, inhibit the PI3K, Ras and ERK signaling pathways, limit T-cell/dendritic cell (DC)-dwell time and promote expression of the inhibitory transcription factor BATF (1). More recently, Hui et al (2) showed that CD28 is the primary target of PD-1-recruited SHP-2, suggesting that PD-1 inhibits T-cell function through inactivation of CD28 signaling. The transient upregulation of PD-1 during T-cell activation and its maintenance at high levels on chronically-stimulated (exhausted) T cells, enable PD-1 to negatively regulate T-cell function during priming, secondary activation and in conditions of prolonged antigen exposure (1, 3, 4). Furthermore, PD-1 is expressed on a large proportion of tumor-infiltrating T cells, yet even within this population PD-1 expression is skewed towards the tumor-reactive, and presumably chronically stimulated, subpopulation (1, 5).

Encouragingly, countering PD-1 with PD-1- or PD-L1-specific monoclonal antibodies (mAb) enables functional CD8+ T cells to accumulate, leading to tumor rejection in pre-clinical models and dramatically improved outcomes across a range of cancer types in patients. Despite these unprecedented clinical successes, response rates remain modest and rarely

exceed 40% (6). Reasons for the observed patient variability to PD-1/L1 blockade are doubtless multifactorial, but the extent of CD8+ T-cell infiltration is likely to be an important factor in the resistance to immunotherapy (7). Recent findings demonstrate that the lack of T-cell infiltration is the result of defective recruitment and activation of DCs, which leads to reduced cross-priming of CD8+ T cells (8). Based on these findings, a number of studies have shown that the intra-tumoral administration of inflammatory mediators alone or together with DCs can result in T-cell priming and improved anti-tumor immunity (8). However, the broad applicability of this approach, particularly for the treatment of metastatic disease, is likely to be limited. We and others have previously demonstrated that DC expression of CD70, the ligand for CD27, is required for efficient priming of CD8+ T cells and effective anti-tumor immunity in murine models (9-14). Furthermore, we have shown that the requirement for DC activation can be largely replaced by systemic administration of soluble recombinant CD70 or agonist anti-CD27 mAb (12, 14, 15). We reasoned that the ability of CD27 agonists to enhance CD8+ T-cell priming could combine with PD-1 blockade to further improve CD8+ T-cell responses and anti-tumor immunity. Indeed we have shown previously in a CD4-independent model of donor lymphocyte infusion in which CD8+ T cells are exhausted by continued exposure to antigen, that transient CD8+ T-cell reinvigoration can be achieved by the combination of agonist anti-CD27 and anti-PD-L1 (16). In contrast however, others have reported that agonist anti-CD27 and PD-1 blockade fails to synergize for improved CD8+ T-cell accumulation in a CD4-independent DNA vaccination model (17).

We here clarify these discrepant findings and demonstrate that agonist anti-CD27 mAb is synergistic with PD-1/L1 blockade in promoting CD8+ T-cell expansion, function and tumor protection in multiple models. Functionally, we find that anti-CD27 and PD-1/L1 blockade co-operate to drive proliferative and cytotoxic gene expression programs in CD8+ T cells.

These data reveal the complex interplay between co-stimulatory and inhibitory receptors in regulating T-cell activation and provide new impetus for evaluating combined agonist anti-CD27 and PD-1/L1 blockade in patients.

Materials and Methods

Cell lines and reagents

The cell lines B16-OVA-GFP, B16-BL6, FVAX and C1498 have all been described previously (18-20) and were maintained in Dulbecco's modified Eagles Medium containing 10% FCS, pyruvate, L-glutamine and antibiotics. Stocks of cells were maintained in liquid nitrogen. Defrosted cells were discarded within 3 months and regularly visualized for any changes in morphology or growth rate. Cell lines were routinely tested for mycoplasma contamination using endosafe-PTS cartridges (Charles River). BCL1 tumor was maintained by passage in BALB/c mice as described (21). Endotoxin-low peptides $hgp100_{25\text{-}33}$ (KVPRNQDWL), $OVA_{257\text{-}264}$ (SIINFEKL) and the altered peptide ligand SIIQFEKL were obtained from Peptide Protein Research Ltd. Cyclophosphamide and FTY720 were obtained from Sigma Aldrich and Cell Proliferation Dye eFluor450 and Fixable Viability Dye eFluor506 were from eBioscience. PE-labeled SIINFEKL peptide/H-$2K^b$ tetramers were manufactured in house (Protein Core Facility). Antibodies used in vivo were rat anti-mouse CD27 (AT124; rat IgG2a), anti-OX40 (OX-86), anti-GITR (DTA-1), anti-4-1BB (LOB12.3), anti-CD4 (GK1.5 and YTA3.1.2), anti-CD8 (YTS169), rat IgG2a isotype control antibodies Mc106A5 or Mc39-16 (all prepared <10 EU/mg endotoxin in house); anti-mouse PD-1 (RMP1-14), anti-mouse PD-L1 (10F.9G2) and rat IgG2b isotype control mAbs were obtained from Bio X cell. Anti-human CD27 mAb, varlilumab, has been described previously (21).

Mice and in vivo protocols

C57BL/6, BALB/c, OT-I, pmel1 and hCD27-Tg mice have been described previously (21, 22). Experiments were conducted according to U.K. Home Office Regulations or according to the guidelines established by the Institutional Animal Care and Use Committee (IACUC)

at Celldex Therapeutics, Inc. For adoptive CD8+ T-cell transfer, single cell suspensions of splenocytes were prepared in phosphate buffered saline (PBS) and 1-5x10^6 CD8+Vβ13+Thy1.1+ cells (pmel1) or 1x10^4 CD8+SIINFEKL/H-2K^b tetramer+ (OT-I) cells were injected intravenously (i.v.). For tumor challenge, adherent cell lines were treated with trypsin-EDTA, washed and viable cells counted and injected into mice. C1498 cells were washed and counted prior to i.v. injection. BCL1 cells were maintained by in vivo passage and hCD27-Tg mice challenged with 1x10^7 cells i.v. For in vivo depletion experiments, mice received a total of 3mg anti-CD4 antibody (a 50/50 mix of GK1.5 and YTA3.1.2) or a minimum total of 1.5mg anti-CD8 (clone YTS169) split over three intra-peritoneal (i.p.) injections between days -7 and +4 relative to tumor challenge. FVAX cells were treated with trypsin-EDTA, washed in PBS and irradiated (208 Gy) prior to sub-cutaneous (s.c.) injection on the opposite flank to that of live B16-BL6 cells, on days 3, 6 and 9 relative to tumor challenge. For in vivo blockade of IL-2, mice were treated i.p. on days 0, 1 and 2 relative to peptide vaccination, with a mix of anti-IL-2 mAbs JES6-1A12 (50μg/day; Bio X Cell) and S4B6.1 (200μg/day; in house) as reported previously (23). For FTY720 treatment, mice were treated i.p. on alternate days with 50μg drug in 200μl PBS/2.5% DMSO prepared fresh, or with PBS/DMSO as a control.

Flow cytometry

Antibodies used for flow cytometry were anti-Thy1.1-APC or -eFluor450 (HIS51), anti-CD8α-FITC, -APC or -APC-Cy7 (53-6.7), anti-CD4-FITC, -eFluor450 or -APC (GK1.5), anti-OX40-PE (OX86), anti-CD27-PE (LG.3A10), anti-GITR-PE (DTA-1), anti-4-1BB-PE (17B5), anti-PD-1-APC (J43), anti-Vβ13-FITC (MR12.3), anti-CD107a-eFluor450 (eBio104B), anti-T-bet-FITC (eBio4B10), anti-IFN-γ-APC (XMG1.2), anti-TNF-α-FITC

(MP6-XT22), anti-IL-2-PE (JES6-5H4), anti-Foxp3-PE (FJK-16s), anti-CD25-PE (PC61.5) and appropriate isotype controls (all from eBioscience) as well as anti-granzyme B-APC (GB11; Invitrogen), anti-CD8-PE (YTS169; in house), anti-Myc-AlexaFluor647 (D84C12; Cell Signaling Technology), anti-Stat5(pY694)-AlexaFluor647 (47/Stat5; BD Biosciences) and appropriate isotype controls. For analysis of tumor infiltrating lymphocytes (TILs), tumors were passed through a 70μm mesh and mononuclear cells isolated by density gradient centrifugation prior to flow cytometric staining.

For all flow cytometry, cells were incubated with 10μg/ml anti-Fc receptor mAb (2.4G2; in house) for 10 mins prior to surface staining. For subsequent intracellular staining of T-bet, Foxp3, granzyme B and Myc, cells were treated using the Foxp3/transcription factor buffer staining set (eBioscience). For detection of surface CD107a, splenocytes were restimulated for 4 hours with 1μM relevant or control peptide and either anti-CD107a-eF450 or an isotype control in the presence of Golgistop (BD Pharmingen) prior to re-surface staining for CD107a and other surface markers as indicated. For the detection of intracellular cytokines, splenocytes were re-stimulated for 4-5 hours with 1μM relevant or control peptide in the presence of Golgiplug (BD Pharmingen) prior to surface staining, fixation in 1% formaldehyde/PBS and intracellular cytokine staining in 0.5% saponin/PBS. For the detection of intracellular Stat5(pY694), splenocytes were restimulated ex vivo with 20U/ml IL-2 for 15 mins prior to surface staining for CD8 and Thy1.1, fixation (Cytofix/Cytoperm kit; BD), treatment with ice-cold methanol for 30 mins and intracellular staining for 30 mins (Cytofix/Cytoperm kit). Flow cytometry was performed on a FACsCalibur using BD Cellquest software or on a FACsCantoII using BD FACsDiva software. FCS Express V3 was used for figure preparation.

Microarray analysis

For transcriptome analysis mice received $2x10^6$ pmel1 CD8+ T cells prior to i.v. injection of 100μg hgp100 peptide and 400μg total IgG comprised of 200μg anti-CD27, 100μg anti-PD-1, 100μg anti-PD-L1 or isotype control mAbs to make up the total IgG dose. Splenocytes were collected on day 4 relative to immunization, CD8+ T cells isolated by negative selection (CD8+ T cell isolation kit; Miltenyi Biotech) and CD8+Thy1.1+ cells positively sorted on a FACsAria to >99% purity. A minimum of $0.4x10^6$ cells were collected, RNA extracted using RNeasy kits and gDNA eliminator columns (Qiagen) and stored at -80^oC. Samples were analyzed on an Affymetrix Mouse Transcriptome Array 1.0 (AROS Applied Biotechnology, Denmark). Raw microarray data were quantile-normalized using the Bioconductor R package "oligo". Genes were tested for differential expression using an empirical Bayes moderated t-test as implemented in the limma R package (version 3.30.9). The moderated t-statistic was calculated for each gene and p-values were corrected for multiple testing across genes and contrasts using the decideTests function (adjustment method = 'separate'). The threshold for significant differential expression was a false discovery rate of $q<0.05$. Subsequent data analysis used Ingenuity Pathway Analysis (IPA; Qiagen).

Statistical analysis

Experimental statistical analyses were performed using GraphPad Prism software. Student's two-tailed t-test, Log-rank (Mantel-Cox) test and two-way ANOVA (with Bonferroni's *post hoc* test) were used throughout as indicated in the text. Data were considered significant at $p<0.05$.

Data availability

Experimental datasets generated during this study are available from the corresponding author upon reasonable request. Data generated from the microarray have been uploaded to the NCBI Gene Expression Omnibus and are available as GSE96923.

Results

Anti-CD27 is superior to other anti-TNFRSF mAb for CD8+ T-cell expansion in vivo

With the ultimate aim of combining an effective TNF receptor superfamily (TNFRSF) agonist with PD-1 blockade, we initially compared several agonist anti-TNFRSF mAb for their ability to augment CD8+ T-cell expansion. To this end, gp100-specific CD8+ T cells from pmel1 transgenic mice were adoptively transferred to congenic recipients prior to injection of peptide alone or with agonist mAb as indicated. Human gp100 peptide (hgp100) is approximately 100-fold more potent than murine gp100 in stimulating pmel1 CD8+ T cells (22, 24) and therefore hgp100 peptide was used for this, and all subsequent, experiments. Within the limited panel of mAb evaluated all mAb are known T-cell agonists (12, 25, 26), yet in this setting only anti-CD27 mAb was able to significantly expand pmel1 CD8+ T-cells compared with hgp100 peptide alone (Supp. Fig. S1A). Analysis of TNFRSF receptor expression on CD8+ pmel1 T cells (Supp. Fig. S1B) confirmed that resting CD8+ T cells express CD27 and GITR but not OX40 or 4-1BB, in line with previous publications (27, 28). OX40 and 4-1BB were both upregulated at 48 hours, but expression of these receptors was still relatively low compared with expression of CD27 and GITR at the same time point. Importantly, we noted that stimulation of pmel1 CD8+ T cells with peptide alone was sufficient to cause upregulation of the inhibitory PD-1 receptor and PD-1 remained on pmel1 cells after stimulation with peptide and anti-CD27 (Supp. Fig. S1C).

Optimal CD8+ T-cell expansion and differentiation into effector cells requires CD27 costimulation and PD-1/L1 blockade

To assess if PD-1 expression on activated CD8+ T cells limits the activity of agonist anti-CD27, we examined the effect of combining agonist anti-CD27 with blockade of the PD-1/L1 pathway on T-cell priming. Data shown in Fig. 1 reveal that the effects of combined treatment on pmel1 T-cell expansion are indeed synergistic. Thus, while T-cell proliferation, determined by cell-proliferation dye dilution, was induced by anti-CD27 and anti-PD-1/PD-L1, it was more extensive following the combination treatment (Fig 1A, *top and bottom-left panels*). Enumerating pmel1 T cells in the spleen revealed that while anti-CD27 and anti-PD-1/L1 produced an increase in pmel1 cells of 17-fold and 6-fold respectively compared with peptide alone, the combination treatment resulted in a 64-fold increase in pmel1 CD8+ T-cell number (Fig. 1A, *bottom-right panel*). The enhanced expansion afforded by the combination treatment was not limited to pmel1 T cells and was also evident after stimulation of OT-I transgenic CD8+ T cells with either high- or low-affinity ovalbumin-derived peptides (Supp. Fig. S2A and B).

Furthermore, combination treatment, but not anti-CD27 or anti-PD-1/L1 alone, increased expression of the T-box transcription factor T-bet (Fig. 1B), a key positive regulator of T-cell effector function and IFN-γ synthesis (29). In addition, combination-activated CD8+ T cells revealed a more effector-like phenotype with significantly higher levels of intracellular granzyme B, surface CD107a, a surrogate marker of degranulation (Fig. 1B), and of intracellular IFN-γ and TNF-α (Fig. 1C) compared with cells treated with either anti-CD27 or anti-PD-1/PD-L1 alone. Consistent with previous findings by us and others in which IL-2 transcription was identified as a major output of CD27 activation in T cells (15, 30), anti-CD27 significantly increased IL-2 production compared with peptide alone and this could not be further amplified by PD-1/L1 blockade (Fig. 1C). Finally, combined anti-CD27 and PD-

1/L1 blockade also significantly increased the frequency of polyfunctional CD8+ T cells such that 41% of cells produced 2 or 3 cytokines after combination treatment compared with only 25% of anti-CD27 treated and <3% of anti-PD-1/L1-treated cells (Fig. 1D; $p<0.02$, Student's t-test). Overall these data demonstrate that many of the costimulatory effects of agonist anti-CD27 during priming are dampened by inhibitory PD-1 signaling and that the combination of PD-1 blockade and CD27 costimulation can massively boost CD8+ T-cell priming compared with either treatment alone.

Combined agonist anti-CD27 and PD-1 blockade activates a distinct gene expression program in CD8+ T cells

To investigate the mechanism(s) through which agonist anti-CD27 and PD-1/L1 blockade combine to enhance CD8+ T-cell expansion and function, adoptively transferred CD8+Thy1.1+ pmel1 cells were stimulated with peptide and mAb in vivo (either anti-PD-1/L1 or anti-CD27 alone or in combination) and purified at the peak of the response (Supp. Fig. S3), prior to transcriptome analysis by microarray. Minimal expansion of pmel1 cells after injection of peptide alone precluded inclusion of this group. After normalization, two-dimensional unsupervised clustering was used to generate a heatmap showing gene-expression differences for the shared set of genes exhibiting significant changes in expression between both of the monotherapy groups and the combination-treated group (418 genes) and the smaller gene set (174 genes) whose expression was significantly changed between the highest-performing monotherapy (anti-CD27) and the combination group (Fig. 2A). We considered that these genes were most likely to be responsible for the synergistic effects of anti-CD27 and PD-1/L1 blockade given that anti-CD27 alone was the most effective of the monotherapies. The heatmap therefore represented 592 genes in which gene expression

patterns tightly clustered into the three experimental groups, demonstrating minimal within-group variation.

Six clusters of gene expression were observed, with clusters 3 and 4 representing genes upregulated in the combination group compared with either anti-CD27 or anti-PD-1/PD-L1 single treatment (Fig. 2A). These genes were either predominantly driven by anti-CD27 (cluster 3; 254 genes) or anti-PD-1/L1 (cluster 4; 120 genes) and overall both clusters were enriched for genes encoding proteins with a role in DNA replication and cell proliferation (Fig. 2B and C). Closer scrutiny (Supp. Table S1) revealed that cluster 3 also included genes encoding the T-cell effector/memory differentiation transcription factors Id2 and Eomes as well as genes encoding enzymes driving glycolysis (*Pgam1, Pfkp*), glutaminolysis (*Ppat*) and fatty acid and cholesterol synthesis (*Lss, Acaca, Fads1, Dhcr24*). Cluster 4 also included genes involved in these metabolic pathways (e.g. *Tpi1, Fads2* and *Fdps)*, yet only cluster 4 and not cluster 3, additionally contained genes linked to cytotoxic function ($p=1.44x10^{-10}$, $z=1.764$) including genes encoding granzymes A, B and K and killer cell lectin-like receptors NKG2A, NKG2C, NKG2D and NKG2E (Fig. 2C and Supp. Tables S1 and S2). Furthermore, cluster 4 incorporated additional genes associated with effector CD8+ T cells including receptors for key cytokines (IL-2 and IL-12) and *Tbx21*, which encodes T-bet (Fig. 2C and Supp. Table S2). Comparison of the genes in clusters 3 and 4 which exhibited the greatest fold change between single treatment and combination groups also revealed a bias towards genes controlling cell proliferation and T-cell effector function in clusters 3 and 4 respectively (Supp. Table S2). The top functional networks for each of clusters 3 and 4 (Fig. 2B and C respectively) and normalized expression values for each of the granzymes in cluster 4 (Fig. 2D) are shown. Together these data indicate that anti-CD27 and PD-1/L1 blockade

co-operate to control a pro-proliferative and cytotoxic gene expression program that culminates in enhanced T-cell expansion and effector function.

Analysis of the transcription factors that promote expression of genes in clusters 3 and 4 revealed Myc and E2F1 to be highly significant regulators of both gene clusters (Fig. 3A-D). Myc is a key driver of T-cell proliferation and growth (31, 32) and E2F1 together with E2F2 control homeostatic T-cell proliferation (33). In support of a key role for Myc in facilitating CD8+ T-cell activation, combination-treated CD8+ T cells expressed higher levels of Myc protein, compared with monotherapy-treated, CD8+ T cells (Fig. 3E and F). Furthermore, previous reports have shown that maintenance of Myc in activated T cells is dependent on IL-2 signaling and amino-acid uptake, such that expression of the IL-2-receptor alpha chain CD25 and the prevalence of amino-acid transporter Slc7a5 transcripts correlate with Myc expression (34, 35). Our finding that CD25 protein, phosphorylation of the downstream-signaling moiety Stat5, and the prevalence of Slc7a5 transcripts are significantly elevated in cells treated with combined anti-CD27 and PD-1/L1 blockade treatment compared with monotherapy-treated cells (Fig. 4A-E), suggests that these factors could have combined to enhance Myc expression. Furthermore, in vivo blockade of IL-2 significantly reduced the expansion of CD8+ T cells after combined anti-CD27 and PD-1/L1 blockade (Fig. 4F), and hindered acquisition of effector proteins as evidenced by almost complete abrogation of granzyme B expression and significant reductions in the production of IFN-γ and TNF-α (Fig. 4G-I).

Gene expression changes in the remaining clusters of the heatmap were also largely consistent with the superior effector phenotype of CD8+ T cells treated with combination

therapy (Supp. Table S1). For instance, combination-induced genes in cluster 2 that showed increased expression when compared to anti-CD27 and comparable expression to anti-PD-1/L1, included the pro-effector CD8+ T-cell gene, *Rheb* (36), and *Ctla2a* and *Ctla2b*, putative cysteine protease-like molecules (37). Similarly, in cluster 1, several T-cell inhibitory genes exhibited decreased expression after combination treatment compared with either monotherapy treatment e.g. *Rgs10*, which limits Vav1-Rac1 activation and T-cell adhesion (38), *Itm2c*, a mediator of cell death downstream of TNF-α (39) and *Spry1*, an inhibitor of CD8+ T-cell cytotoxicity (40). Furthermore, expression of *Id3*, which encodes a fate-determining transcription factor downregulated in effector CD8+ T cells (41), was also decreased in combination-treated CD8+ T cells in cluster 1.

A large number of genes in the heatmap (183/592) showed greatest expression after anti-CD27 treatment alone. For this gene cohort, inclusion of PD-1/L1 blockade inhibited expression to a level between that induced by each monotherapy (cluster 5), or to a baseline lower than either monotherapy (cluster 6). Consistent with an intermediate expression profile by combination-treated CD8+ T cells, cluster 5 genes included those with both positive (e.g. *Rel*, *Lef1* (42, 43)) and negative (e.g *TNFAIP3*, *CD274* (1, 44)) influences on effector CD8+ T-cell proliferation and/or function. Genes represented in cluster 6 were diverse in function yet included *Mir15b*, *Rgcc* and *Ctla4*, all inhibitors of T-cell cytokine production and/or proliferation (45, 46), consistent with their preferential suppression in combination-treated CD8+ T cells. A full list of the genes represented in each cluster can be found in Supp. Table S1.

Agonist anti-CD27 and PD-1/L1 blockade synergize for improved adoptive T-cell therapy (ACT)

To ascertain whether the increase in CD8+ T-cell frequency and effector function seen after combined anti-CD27 and PD-1 blockade treatment translates into increased control of tumor, mice were challenged with a lethal dose of B16-BL6 melanoma cells and tumor allowed to establish prior to ACT of pmel1 CD8+ T cells and vaccination with peptide alone, with anti-CD27, anti-PD-1/L1 or with all three mAb together. While neither anti-CD27 nor anti-PD-1/L1 had any substantial impact on tumor growth, combining anti-CD27 and anti-PD-1/L1 delayed tumor growth and significantly improved long-term survival (Fig. 5A and B). Experiments in which anti-PD-1 was used in place of the anti-PD-1/L1 cocktail similarly showed synergy between anti-PD-1 and anti-CD27 for tumor therapy (Supp. Fig. S4A and B). Furthermore, the benefit of combined anti-CD27 and PD-1 blockade was only apparent when mAb were delivered with ACT confirming the CD8+ T-cell dependent nature of the treatment (Supp. Fig. S4C).

Agonist anti-CD27 and PD-1/L1 blockade synergize for enhanced endogenous anti-tumor CD8+ T-cell responses

We next sought to test whether this dual targeting strategy could promote endogenous anti-tumor immunity. To this end mice were challenged with the more immunogenic B16-OVA-GFP tumor prior to mAb injection, in the absence of ACT. Again, anti-CD27 and PD-L1 blockade together synergized to impair tumor growth and significantly improve long-term survival, in marked contrast to monotherapy with either anti-CD27 or anti-PD-L1, which alone had little impact on survival (Fig. 6A and B). Therapy with combined anti-CD27 and anti-PD-L1 was entirely dependent on endogenous CD8+ T cells, but not on CD4+ T cells

(Fig. 6C) consistent with an increased frequency of CD8+ T cells in the tumor after combination treatment (Fig. 6D). Even in an aggressive model of melanoma in which treatment needs to be combined with a cellular vaccine, the combination of anti-CD27 and anti-PD-L1, but neither agent alone, significantly retarded tumor growth (Supp. Fig. S5A) and synergized to enhance accumulation of local CD8+ T cells (Supp. Fig. S5B). Furthermore, blocking lymphocyte egress from lymph nodes in mice bearing small established tumors had no detrimental effect on tumor therapy driven by anti-CD27 and PD-1/L1 blockade suggesting direct activation of tumor-resident T cells (Fig. 6E and F). To determine whether the synergy between anti-CD27 and PD-1 blockade was applicable to tumor types other than melanoma, we also evaluated this approach in a model of acute myeloid leukaemia. Similarly, only the combination of anti-CD27 and PD-1 blockade, and neither therapy alone, conferred significant therapeutic benefit (Fig. 6G). A similar trend towards improved tumor protection by the combination treatment was also observed when mice were treated with mAb in conjunction with chemotherapy (Fig. 6H).

Agonist anti-human CD27 and PD-1/L1 blockade synergize for improved tumor therapy in human CD27 transgenic mice

Finally to move towards clinical translation we evaluated whether a previously described, and clinically relevant, agonistic anti-human CD27 mAb, varlilumab (21), also synergizes with PD-L1 blockade in vivo. Human CD27 transgenic mice (21) were challenged with a lethal dose of BCL1 lymphoma cells prior to injection with varlilumab, anti-PD-L1 or both mAb together in a sub-optimized setting in which varlilumab alone does not show efficacy. In line with our findings across multiple established tumor models in wild-type mice, treatment of human CD27 transgenic (hCD27-Tg) mice with anti-human CD27 mAb or with anti-PD-L1

alone had little impact on tumor growth, yet combined treatment conferred significant long-term protection with over half of the mice surviving longer than 80 days (Fig. 6I).

Discussion

Blockade of the PD-1-PD-L1 pathway in humans has produced significant benefits across multiple types of solid tumors, but response rates remain modest and vary from ~ 15% to 40% depending on the tumor type (47). Recent data indicate that resistance to PD-1 immunotherapy in the non-responding subset is not due to a lack of antigens, but correlates with the absence of CD8+ T cells within the tumor (48). This suggests that strategies that boost the number of infiltrating T cells, for example through augmenting T-cell priming, could improve the therapeutic response of anti-PD-1/L1 mAb. In this study we have started to address this premise by investigating if the combination of agonist anti-CD27 mAb could synergize with blockade of the PD-1 pathway for improved anti-tumor immunity. CD27 is a well-characterized costimulatory receptor for CD8+ T cells and when tested as a monotherapy, agonist anti-CD27 mAb was superior to mAbs targeting other costimulatory receptors such as OX40, 4-1BB and GITR in driving expansion of gp100-specific CD8+ T cells in vivo (Supp. Fig. S1). We show here that the combination of agonist anti-CD27 and anti-PD-1/L1 mAb is indeed synergistic; the combined treatment resulted in improved priming of pmel1 CD8+ T cells as evidenced by increased T-cell proliferation and enhanced differentiation into effector T cells (Fig. 1). Consequently, when compared to monotherapy the combined treatment afforded more robust anti-tumor immunity in a number of pre-clinical tumor models. Furthermore, the observed synergy was not limited to a single anti-CD27 mAb because varlilumab, an anti-human CD27 mAb currently in phase I/II clinical testing, also successfully synergized with PD-1 blockade in augmenting anti-tumor immunity in mice that expressed human CD27.

By characterizing the transcriptomes of pmel1 CD8+ T cells primed under different conditions in vivo we found that anti-CD27 mAb and blockade of PD-1 synergized by reinforcing the expression of genes that regulate cell proliferation and those associated with cytotoxicity of CD8+ T cells. Unexpectedly, the contribution of CD27 triggering and PD-1 blockade was not equivalent with CD27 costimulation exerting a more dominant role in regulating the proliferation program (Fig. 2 and Supp. Table S2). Thus, amongst the 592 genes that were significantly changed in the combination arm compared to each of the monotherapy arms, 114 (19.2%) cell proliferation-associated genes were induced strongly by CD27 costimulation (Fig. 2 and Supp. Tables S1 and S2). In contrast, only 57 genes (9.6%) associated with cell proliferation were differentially induced by PD-1 blockade. We identified Myc as a potential driver of a significant number of genes upregulated by the combination treatment (Fig. 3A-D). Previous reports have shown that the expression of Myc regulates metabolic reprogramming of T cells (31), correlates with expression of IFN-γ and CD69 (34) and regulates the extent of cell proliferation with small changes in Myc resulting in large changes in cell frequency (32). Our data further show that anti-CD27 and PD-1/L1 blockade converge to maximally promote Myc protein levels and a Myc-regulated program of gene expression in vivo. Myc protein has a half-life of around 20 minutes in vivo but can be maintained by IL-2 in a dose-dependent manner such that expression of CD25 correlates with Myc protein levels in T cells (34). Interestingly, our data show CD25 and phosphorylated Stat5 (pY694), a key downstream mediator of IL-2 signaling, to be synergistically increased by anti-CD27 and PD-1/L1 blockade, providing a potential mechanism for co-operative maintenance of Myc by combination treatment, and suggesting that while anti-CD27 drives an increase in IL-2, both anti-CD27 and PD-1 blockade may be required to maximize its capture and downstream signaling. IL-2 maintains Myc predominantly at a post-transcriptional level dependent on amino-acid uptake via Slc7a5,

itself upregulated by IL-2 (34, 35). Consistent with co-operatively upregulated IL-2 signaling, we find that anti-CD27 and PD-1/L1 blockade synergistically increase the frequency of Slc7a5 mRNA transcripts, further supporting an IL-2-driven mechanism of Myc maintenance. Furthermore, blockade of IL-2 significantly hindered the expansion of CD8+ T cells and their acquisition of effector functions, thus supporting our hypothesis that anti-CD27 and PD-1/L1 blockade converge to enhance proliferative and effector differentiation programmes downstream of IL-2 and Myc. However, confirmation of the role of IL-2/Myc in this setting would require in-depth analysis of gene expression at a range of time points, particularly given that maximal Myc expression appears to precede maximal expression of CD25 (Figs 3 and 4).

That we find anti-CD27 and anti-PD-1/L1 to synergize for CD8+ T-cell activation may reflect the influence of PD-1 and CD27 on largely distinct signaling pathways. CD27 uses TRAFs 2 and 5 to engage downstream JNK, and canonical and non-canonical NF-κB pathways leading to high levels of IL-2 transcription (30, 49). In contrast, PD-1 recruits phosphatases to inhibit CD28 and possibly CD3ζ/ZAP70 phosphorylation, limit activation of the PI3K/Akt and Ras/MEK/Erk pathways and upregulate the transcription factor BATF to repress proliferation and IL-2 production (1, 2, 50, 51). Interestingly, PD-1 inhibition synergizes with IL-2 to reinvigorate exhausted T cells during chronic viral infection suggesting that de-repression of IL-2 by PD-1 blockade elicits only sub-optimal concentrations of this cytokine, at least in exhausted T cells (52). Our data similarly show that PD-1 blockade during priming has little effect on IL-2 production by CD8+ T cells suggesting that the ability of anti-CD27 to promote IL-2 might be key to its effective co-operation with anti-PD-1/L1.

Together our data provide clear evidence that agonist anti-CD27 antibodies combine successfully with PD-1/L1 blockade to improve CD8+ T-cell activation, frequency and tumor therapy in a range of settings, and support the ongoing evaluation of agonist anti-CD27 (varlilumab) with PD-1/L1 blockade in patients (NCT02335918). Of note, a recent report has shown that the extent of T-cell reinvigoration following anti-PD-1 treatment determines the likelihood of clinical response in melanoma patients (53) suggesting that combining anti-CD27 mAb with PD-1 blockade may also increase the frequency of responders in the clinic. Finally by defining the mechanism through which CD27 agonism and PD-1 blockade combine for optimal T-cell activation, our work also provides a platform to define biomarkers that predict clinical responses to immunotherapy.

Acknowledgments

The authors would like to thank members of the Biomedical Research Facility for animal husbandry, L. Douglas and P. Duriez of the Cancer Research UK (CRUK) Protein Production Facility for the PE-labeled H-2K^{b}/SIINFEKL tetramer, T. Inzhelevskaya for supplying antibodies for in vivo use and Cancer Research UK for funding.

Author contributions

S.L.B., M.F., V.Y.T., A.R., L.J.T., C.A.P and L-Z.H performed experiments and interpreted the data; S.L.B., S.M.T. and A.A-S. analyzed the transcriptomic data; M.A.C. provided key materials; S.L.B. and A.A-S. wrote the manuscript; T.K. and A.R. revised the manuscript; T.K. and A.A-S. supervised the project.

References

1. Pauken KE, Wherry EJ. Overcoming T cell exhaustion in infection and cancer. Trends Immunol. 2015;36:265-76.
2. Hui E, Cheung J, Zhu J, Su X, Taylor MJ, Wallweber HA, et al. T cell costimulatory receptor CD28 is a primary target for PD-1-mediated inhibition. Science. 2017;355:1428-33.
3. Brown KE, Freeman GJ, Wherry EJ, Sharpe AH. Role of PD-1 in regulating acute infections. Curr Opin Immunol. 2010;22:397-401.
4. Fuse S, Tsai CY, Molloy MJ, Allie SR, Zhang W, Yagita H, et al. Recall responses by helpless memory CD8+ T cells are restricted by the up-regulation of PD-1. Journal of immunology. 2009;182:4244-54.
5. Gros A, Robbins PF, Yao X, Li YF, Turcotte S, Tran E, et al. PD-1 identifies the patient-specific CD8(+) tumor-reactive repertoire infiltrating human tumors. J Clin Invest. 2014;124:2246-59.
6. Chen L, Han X. Anti-PD-1/PD-L1 therapy of human cancer: past, present, and future. The Journal of clinical investigation. 2015;125:3384-91.
7. Blank CU, Haanen JB, Ribas A, Schumacher TN. CANCER IMMUNOLOGY. The "cancer immunogram". Science. 2016;352:658-60.
8. Corrales L, Matson V, Flood B, Spranger S, Gajewski TF. Innate immune signaling and regulation in cancer immunotherapy. Cell Res. 2017;27:96-108.
9. Taraban VY, Rowley TF, Al-Shamkhani A. Cutting edge: a critical role for CD70 in CD8 T cell priming by CD40-licensed APCs. J Immunol. 2004;173:6542-6.
10. Taraban VY, Rowley TF, Tough DF, Al-Shamkhani A. Requirement for CD70 in CD4+ Th cell-dependent and innate receptor-mediated CD8+ T cell priming. J Immunol. 2006;177:2969-75.
11. Taraban VY, Martin S, Attfield KE, Glennie MJ, Elliott T, Elewaut D, et al. Invariant NKT cells promote CD8+ cytotoxic T cell responses by inducing CD70 expression on dendritic cells. J Immunol. 2008;180:4615-20.
12. French RR, Taraban VY, Crowther GR, Rowley TF, Gray JC, Johnson PW, et al. Eradication of lymphoma by CD8 T cells following anti-CD40 monoclonal antibody therapy is critically dependent on CD27 costimulation. Blood. 2007;109:4810-5.
13. Bak SP, Barnkob MS, Bai A, Higham EM, Wittrup KD, Chen J. Differential requirement for CD70 and CD80/CD86 in dendritic cell-mediated activation of tumor-tolerized CD8 T cells. Journal of immunology. 2012;189:1708-16.
14. Taraban VY, Rowley TF, Kerr JP, Willoughby JE, Johnson PM, Al-Shamkhani A, et al. CD27 costimulation contributes substantially to the expansion of functional memory CD8(+) T cells after peptide immunization. Eur J Immunol. 2013;43:3314-23.
15. Rowley TF, Al-Shamkhani A. Stimulation by soluble CD70 promotes strong primary and secondary CD8+ cytotoxic T cell responses in vivo. J Immunol. 2004;172:6039-46.
16. Buchan SL, Manzo T, Flutter B, Rogel A, Edwards N, Zhang L, et al. OX40- and CD27-mediated costimulation synergizes with anti-PD-L1 blockade by forcing exhausted CD8+ T cells to exit quiescence. Journal of immunology. 2015;194:125-33.
17. Ahrends T, Babala N, Xiao Y, Yagita H, van Eenennaam H, Borst J. CD27 Agonism Plus PD-1 Blockade Recapitulates CD4+ T-cell Help in Therapeutic Anticancer Vaccination. Cancer Res. 2016;76:2921-31.
18. Sancho D, Mourao-Sa D, Joffre OP, Schulz O, Rogers NC, Pennington DJ, et al. Tumor therapy in mice via antigen targeting to a novel, DC-restricted C-type lectin. The Journal of clinical investigation. 2008;118:2098-110.
19. Curran MA, Montalvo W, Yagita H, Allison JP. PD-1 and CTLA-4 combination blockade expands infiltrating T cells and reduces regulatory T and myeloid cells within B16 melanoma tumors. Proceedings of the National Academy of Sciences of the United States of America. 2010;107:4275-80.

20. Boyer MW, Orchard PJ, Gorden KB, Anderson PM, McLvor RS, Blazar BR. Dependency on intercellular adhesion molecule recognition and local interleukin-2 provision in generation of an in vivo CD8+ T-cell immune response to murine myeloid leukemia. Blood. 1995;85:2498-506.
21. He LZ, Prostak N, Thomas LJ, Vitale L, Weidlick J, Crocker A, et al. Agonist anti-human CD27 monoclonal antibody induces T cell activation and tumor immunity in human CD27-transgenic mice. J Immunol. 2013;191:4174-83.
22. Overwijk WW, Theoret MR, Finkelstein SE, Surman DR, de Jong LA, Vyth-Dreese FA, et al. Tumor regression and autoimmunity after reversal of a functionally tolerant state of self-reactive CD8+ T cells. The Journal of experimental medicine. 2003;198:569-80.
23. Willoughby JE, Kerr JP, Rogel A, Taraban VY, Buchan SL, Johnson PW, et al. Differential impact of CD27 and 4-1BB costimulation on effector and memory CD8 T cell generation following peptide immunization. J Immunol. 2014;193:244-51.
24. Overwijk WW, Tsung A, Irvine KR, Parkhurst MR, Goletz TJ, Tsung K, et al. gp100/pmel 17 is a murine tumor rejection antigen: induction of "self"-reactive, tumoricidal T cells using high-affinity, altered peptide ligand. The Journal of experimental medicine. 1998;188:277-86.
25. Taraban VY, Rowley TF, O'Brien L, Chan HT, Haswell LE, Green MH, et al. Expression and costimulatory effects of the TNF receptor superfamily members CD134 (OX40) and CD137 (4-1BB), and their role in the generation of anti-tumor immune responses. Eur J Immunol. 2002;32:3617-27.
26. Lin GH, Snell LM, Wortzman ME, Clouthier DL, Watts TH. GITR-dependent regulation of 4-1BB expression: implications for T cell memory and anti-4-1BB-induced pathology. Journal of immunology. 2013;190:4627-39.
27. Snell LM, Lin GH, Watts TH. IL-15-dependent upregulation of GITR on CD8 memory phenotype T cells in the bone marrow relative to spleen and lymph node suggests the bone marrow as a site of superior bioavailability of IL-15. Journal of immunology. 2012;188:5915-23.
28. Croft M, Duan W, Choi H, Eun SY, Madireddi S, Mehta A. TNF superfamily in inflammatory disease: translating basic insights. Trends Immunol. 2012;33:144-52.
29. Sullivan BM, Juedes A, Szabo SJ, von Herrath M, Glimcher LH. Antigen-driven effector CD8 T cell function regulated by T-bet. Proceedings of the National Academy of Sciences of the United States of America. 2003;100:15818-23.
30. Peperzak V, Xiao Y, Veraar EA, Borst J. CD27 sustains survival of CTLs in virus-infected nonlymphoid tissue in mice by inducing autocrine IL-2 production. J Clin Invest. 2010;120:168-78.
31. Wang R, Dillon CP, Shi LZ, Milasta S, Carter R, Finkelstein D, et al. The transcription factor Myc controls metabolic reprogramming upon T lymphocyte activation. Immunity. 2011;35:871-82.
32. Heinzel S, Binh Giang T, Kan A, Marchingo JM, Lye BK, Corcoran LM, et al. A Myc-dependent division timer complements a cell-death timer to regulate T cell and B cell responses. Nature immunology. 2017;18:96-103.
33. DeGregori J. E2F and cell survival: context really is key. Dev Cell. 2005;9:442-4.
34. Preston GC, Sinclair LV, Kaskar A, Hukelmann JL, Navarro MN, Ferrero I, et al. Single cell tuning of Myc expression by antigen receptor signal strength and interleukin-2 in T lymphocytes. EMBO J. 2015;34:2008-24.
35. Sinclair LV, Rolf J, Emslie E, Shi YB, Taylor PM, Cantrell DA. Control of amino-acid transport by antigen receptors coordinates the metabolic reprogramming essential for T cell differentiation. Nature immunology. 2013;14:500-8.
36. Velica P, Zech M, Henson S, Holler A, Manzo T, Pike R, et al. Genetic Regulation of Fate Decisions in Therapeutic T Cells to Enhance Tumor Protection and Memory Formation. Cancer Res. 2015;75:2641-52.
37. Denizot F, Brunet JF, Roustan P, Harper K, Suzan M, Luciani MF, et al. Novel structures CTLA-2 alpha and CTLA-2 beta expressed in mouse activated T cells and mast cells and homologous to cysteine proteinase proregions. Eur J Immunol. 1989;19:631-5.

38. Garcia-Bernal D, Dios-Esponera A, Sotillo-Mallo E, Garcia-Verdugo R, Arellano-Sanchez N, Teixido J. RGS10 restricts upregulation by chemokines of T cell adhesion mediated by alpha4beta1 and alphaLbeta2 integrins. Journal of immunology. 2011;187:1264-72.
39. Wu H, Liu G, Li C, Zhao S. bri3, a novel gene, participates in tumor necrosis factor-alpha-induced cell death. Biochem Biophys Res Commun. 2003;311:518-24.
40. Collins S, Waickman A, Basson A, Kupfer A, Licht JD, Horton MR, et al. Regulation of CD4(+) and CD8(+) effector responses by Sprouty-1. PLoS One. 2012;7:e49801.
41. Omilusik KD, Shaw LA, Goldrath AW. Remembering one's ID/E-ntity: E/ID protein regulation of T cell memory. Curr Opin Immunol. 2013;25:660-6.
42. Zhou X, Xue HH. Cutting edge: generation of memory precursors and functional memory CD8+ T cells depends on T cell factor-1 and lymphoid enhancer-binding factor-1. Journal of immunology. 2012;189:2722-6.
43. Bronk CC, Yoder S, Hopewell EL, Yang S, Celis E, Yu XZ, et al. NF-kappaB is crucial in proximal T-cell signaling for calcium influx and NFAT activation. Eur J Immunol. 2014;44:3741-6.
44. Giordano M, Roncagalli R, Bourdely P, Chasson L, Buferne M, Yamasaki S, et al. The tumor necrosis factor alpha-induced protein 3 (TNFAIP3, A20) imposes a brake on antitumor activity of CD8 T cells. Proceedings of the National Academy of Sciences of the United States of America. 2014;111:11115-20.
45. Zhong G, Cheng X, Long H, He L, Qi W, Xiang T, et al. Dynamically expressed microRNA-15b modulates the activities of CD8+ T lymphocytes in mice with Lewis lung carcinoma. J Transl Med. 2013;11:71.
46. Tegla CA, Cudrici CD, Nguyen V, Danoff J, Kruszewski AM, Boodhoo D, et al. RGC-32 is a novel regulator of the T-lymphocyte cell cycle. Exp Mol Pathol. 2015;98:328-37.
47. Topalian SL, Drake CG, Pardoll DM. Immune checkpoint blockade: a common denominator approach to cancer therapy. Cancer Cell. 2015;27:450-61.
48. Spranger S, Luke JJ, Bao R, Zha Y, Hernandez KM, Li Y, et al. Density of immunogenic antigens does not explain the presence or absence of the T-cell-inflamed tumor microenvironment in melanoma. Proc Natl Acad Sci U S A. 2016;113:E7759-E68.
49. Croft M. The role of TNF superfamily members in T-cell function and diseases. Nat Rev Immunol. 2009;9:271-85.
50. Wherry EJ, Kurachi M. Molecular and cellular insights into T cell exhaustion. Nature reviews Immunology. 2015;15:486-99.
51. Kamphorst AO, Wieland A, Nasti T, Yang S, Zhang R, Barber DL, et al. Rescue of exhausted CD8 T cells by PD-1-targeted therapies is CD28-dependent. Science. 2017;355:1423-7.
52. West EE, Jin HT, Rasheed AU, Penaloza-Macmaster P, Ha SJ, Tan WG, et al. PD-L1 blockade synergizes with IL-2 therapy in reinvigorating exhausted T cells. The Journal of clinical investigation. 2013;123:2604-15.
53. Huang AC, Postow MA, Orlowski RJ, Mick R, Bengsch B, Manne S, et al. T-cell invigoration to tumour burden ratio associated with anti-PD-1 response. Nature. 2017;545:60-5.

Figure Legends

Figure 1. Agonist anti-CD27 and PD-1/L1 blockade synergize to increase CD8+ T-cell expansion and effector function.

(**A-D**) Groups of 4 C57BL/6 mice were injected with $2x10^6$ pmel1 CD8+Thy1.1+ cells on day -1, with hgp100 peptide and 200μg each of anti-CD27, an equal mix of anti-PD-1 and anti-PD-L1, and/or isotype control antibodies to an equivalent final antibody dose on day 0 and the same antibody cocktails (minus peptide) on day 1. (**A**, *top*) On day 3 the intensity of cell-proliferation dye in blood CD8+Thy1.1+ cells was determined from mice stimulated with peptide alone (filled grey), or with anti-CD27 (grey line), anti-PD-1/L1 mAbs (black line) or both anti-CD27 and anti-PD-1/L1 (thick black line). (**A**, *bottom left*) Mean fluorescence intensity of cell-proliferation dye in CD8+Thy1.1+ cells on day 3 is shown (**A**, *bottom right*) The number of splenic CD8+Thy1.1+ cells was determined on day 4. (**B**) Mean fluorescence intensity of T-bet and granzyme B in ex vivo splenic CD8+Thy1.1+ cells and %CD107a+ of pmel1 cells after brief in vitro restimulation on day 4. (**C**) Representative intracellular IFN-γ, TNF-α and IL-2 staining of CD8+Thy1.1+ cells, and % cytokine-positive of CD8+Thy1.1+ cells on day 4 after brief in vitro restimulation with peptide; lines as (**A**). (**D**) Percentage of CD8+Thy1.1+ cells expressing combinations of IFN-γ, TNF-α and IL-2. Data in (**A**, *left*) are from one experiment; remaining data are from one of a further three similar experiments. Bar graphs in **A-C** show group means +/- SEM. *p<0.05, **p<0.005, ***p<0.0005, ****p<0.0001, two-tailed Student's t-test.

Figure 2. Anti-CD27 and PD-1/L1 blockade synergize to enhance CD8+ T-cell activation at a transcriptional level.

Groups of 3 mice received $2x10^6$ pmel1 CD8+Thy1.1+ T cells prior to injection with hgp100 peptide and anti-CD27, a mix of anti-PD-1 and anti-PD-L1 or all three mAb combined. Four days later RNA from purified splenic pmel1 CD8+ T cells was isolated and subjected to microarray analysis. (**A**) Two-dimensional unsupervised clustering generated a heatmap representing log2 values of relative mRNA expression changes, and data clustered into 6 groups as indicated. (**B** and **C**) The most prevalent functions of genes represented in clusters (**B**) 3 and (**C**) 4 were determined using IPA (*bottom*) and genes associated with the most highly significant process are represented diagrammatically (*top*). Depth of color represents the magnitude of gene-expression change from anti-CD27-stimulated to combination-stimulated cells (red upregulated and green downregulated); arrow/line color symbolizes activation (orange), a gene change that is inconsistent with the downstream molecule (yellow) or that the effect is not predicted (grey); symbol shape gives an indication of function. (**D**) Mean +/- SEM gene-expression values representing the frequencies of gzma, gzmb and gzmk transcripts in each group. (**B** and **C**) p values taken from 'Diseases and Functions' analysis in IPA calculated by Fisher's exact test, (**D**) Benjamini-Hochberg adjusted Student's t-test *$p<0.05$, **$p<0.005$ or as indicated.

Figure 3. Agonist anti-CD27 and PD-1/L1 blockade synergize for increased Myc activity.

Positive upstream regulators of genes represented in clusters (**A**) 3 and (**B**) 4 as identified by IPA; p-values (crosses; right axis) and z-scores (line; left axis) are indicated. Myc and/or E2F1-regulated genes in clusters (**C**) 3 and (**D**) 4 are shown with symbols and colors as Fig. 2. (**E-F**) Groups of mice received pmel1 CD8+ T cells prior to injection of hgp100 peptide and

isotype control antibodies, anti-CD27, anti-PD-1 and anti-PD-L1, or with all three antibodies combined. On (**E**) day 2, or (**F**) the days indicated, the expression of intracellular Myc in splenic Thy1.1+ CD8+ cells was assessed by flow cytometry. (**E**) Representative staining (black line) for Myc on Thy1.1+CD8+ cells stimulated in vivo as indicated; isotype control staining is shown in each case (grey). (**F**) Mean (+/-SEM) % of Myc+ pmel1 CD8+ T cells at each time point combined from 3 independent experiments, each representing one time point. (**A** and **B**) p values calculated by Fisher's exact test performed by IPA. (**F**) Two-way ANOVA with Bonferroni's post-hoc test *p<0.01, ****p<0.0001.

Figure 4. Maximal CD8+ T-cell activation by agonist anti-CD27 and PD-1/L1 blockade is dependent on IL-2.

(**A-D**) Groups of mice received pmel1 CD8+ T cells prior to injection of hgp100 peptide and isotype control antibodies, anti-CD27, anti-PD-1 and anti-PD-L1, or with all three antibodies combined. On day (**A**) 3, (**C** and **D**) 4 or (**B**) the days indicated, the expression of (**A** and **B**) surface CD25 or (**C** and **D**) intracellular Stat5(pY694) on splenic Thy1.1+ CD8+ cells was assessed by flow cytometry. Representative staining (black line) for (**A**) CD25 and (**C**) Stat5(pY694) on Thy1.1+CD8+ cells stimulated in vivo as indicated; isotype control staining is shown in each case (grey). Mean (+/-SEM) % of (**B**) CD25+ and (**D**) Stat5(pY694)+ pmel1 CD8+ T cells. (**E**) Slc7a5 transcript expression from the microarray experiment shown in Fig. 2. (**F-I**) Groups of mice received Thy1.1+pmel1 CD8+ T cells and antibodies as (**A-D**) either alone (no IL-2 block) or were concurrently treated with IL-2 blocking mAbs given starting two hours prior to peptide/activating mAb injection (day 0) and then given additionally on days 1 and 2. (**F**) The frequency of splenic Thy1.1+CD8+ T cells on day 4 and (**G**) the mean fluorescence intensity of intracellular granzyme B staining ex vivo were

determined by flow cytometry. (**H** and **I**) The % of Thy1.1+CD8+ T cells accumulating intracellular IFN-γ and TNF-α was also assessed after brief in vitro restimulation. (**B**) Data are combined from 3 independent experiments, each representing one time point. Two-way ANOVA with Bonferroni's post-hoc test ****p<0.0001. Data in (**C, D** and **F-I**) are from one experiment with 4 mice per group. Students two-tailed t-test; n.s. p>0.05, *p<0.05, **p<0.005, ****p<0.0001. (**E**) Benjamini-Hochberg adjusted Student's t-test *p<0.05, ****p<0.0001.

Figure 5. Agonist anti-CD27 and PD-1/L1 blockade synergize for improved adoptive T-cell therapy.

(**A** and **B**) Groups of 5 C57BL/6 mice were challenged with $2x10^5$ B16-BL6 tumor cells and received $3x10^6$ CD8+Thy1.1+ cells from pmel1 mice 5 days later. Mice were injected the following day with 200μg hgp100 peptide delivered with anti-CD27, anti-PD-1 and anti-PD-L1, with all three antibodies together (combination) or with isotype control mAb and were boosted with these same antibodies a day later. Mice were culled when mean tumor diameter reached 15mm. Data are pooled from 2 experiments. (**A**) shows mean tumor diameter in each group, (**B**) shows % survival over time. (**A**) *p<0.05 2-way ANOVA, (**B**) **p<0.005 Log-rank (Mantel-Cox) test.

Figure 6. Agonist anti-CD27 and PD-1/L1 blockade synergize for enhanced endogenous anti-tumor CD8+ T-cell responses in wild-type and hCD27-Tg mice.

(**A-F**) Groups of mice were challenged with $5x10^5$ B16-OVA-GFP tumor cells s.c. prior to treatment with (**A-C**) 200μg anti-CD27, anti-PD-L1, a combination of the two or with isotype

control mAb delivered i.p. on days 5, 7 and 9. (**C**) Groups of mice additionally received depleting antibodies to CD4 or CD8. (**D**) Frequency of CD8+ T cells within live lymphocytes in B16-OVA-GFP tumor after treatment with the mAbs indicated on days 10, 12 and 14; mice were culled on day 19. In (**E** and **F)** mice were treated with a mix of anti-CD27, anti-PD-1 and anti-PD-L1 or received isotype control antibodies on days 7, 9 and 11 and received i.p. injections of FTY720, or control, every other day from day 6 to day 24 inclusive. Data in (**E**) show percentage of CD8+ (*left*) and CD4+ (*right*) cells of lymphocytes in the blood on day 7 prior to mAb injection. Data in (**F**) show mean tumor growth in each group. (**G** and **H**) Groups of mice were challenged with 10^6 C1498 cells i.v. prior to injection of (**G**) 200μg anti-PD-1, anti-CD27, both together or control antibodies every other day from days 10-20 inclusive, or (**H**) 180mg/kg cyclophosphamide and injection of 150μg antibodies on days 8, 10, 11, 13 and 15. (**I**) Groups of 10 hCD27-Tg mice were challenged with BCL1 tumor cells prior to i.p. injection of 200μg anti-human CD27 on days 4, 6, 8, 10 and 12 and/or 100μg anti-PD-L1 on days 4, 6 and 8. Data in (**B, C** and **G-I**) show % survival to the humane end-point and data are pooled from (**A**, **B, G** and **I**) 3, (**C**) 2 or (**D, E, F** and **H**) 1 independent experiment(s). (**A** and **F**) *p<0.05, **p<0.005, 2-way ANOVA, (**B, C** and **G-I**) **p<0.005, ****p<0.0001, or as indicated, Log-rank (Mantel-Cox) test, (**D** and **E**) **p<0.005, ***p<0.0005, Student's two-tailed t-test.

Figure 1

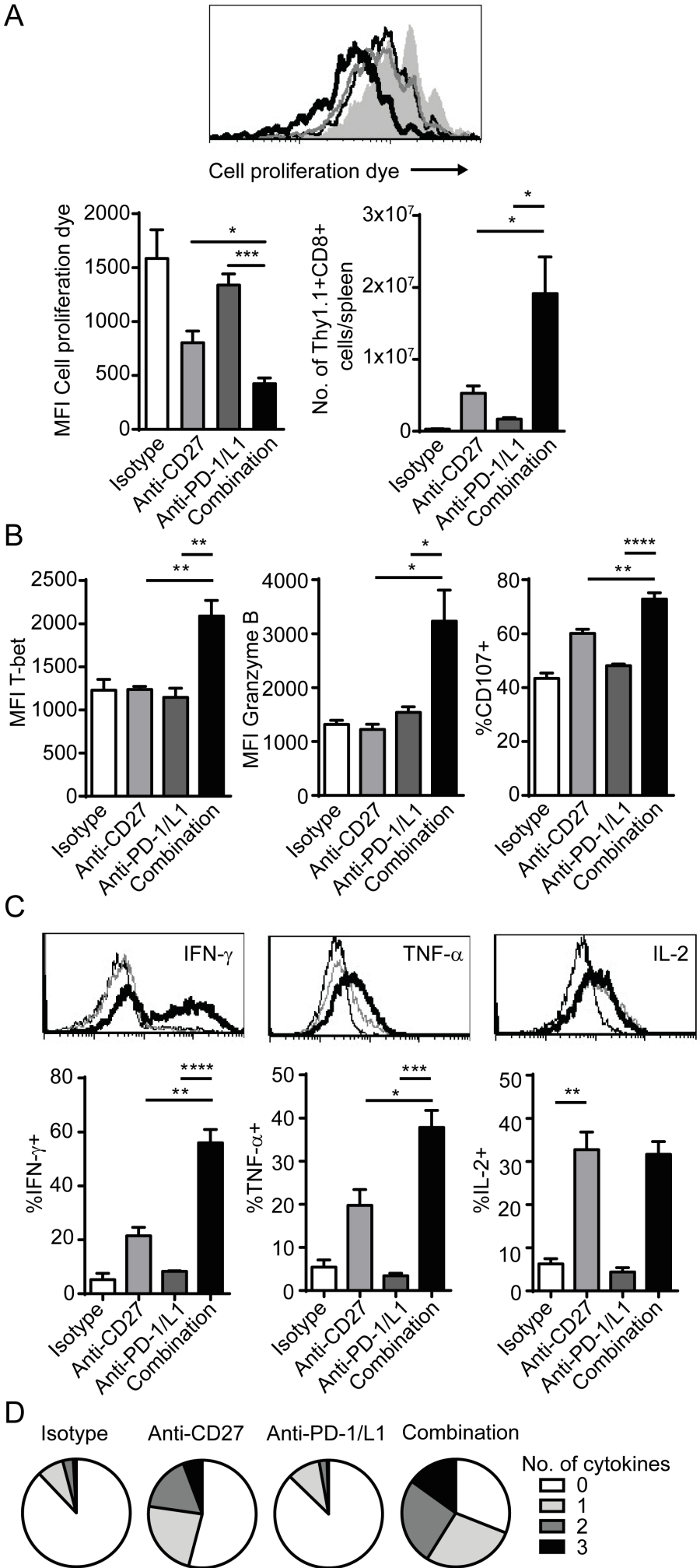
A
Cell proliferation dye
MFI Cell proliferation dye
2000
1500
1000
500
0
*
***
No. of Thy1.1+CD8+ cells/spleen
3x10^7
2x10^7
1x10^7
0
*
*
Isotype
Anti-CD27
Anti-PD-1/L1
Combination
B
MFI T-bet
2500
2000
1500
1000
500
0
**
**
MFI Granzyme B
4000
3000
2000
1000
0
*
*
%CD107+
80
60
40
20
0
****
**
C
IFN-γ
TNF-α
IL-2
%IFN-γ+
80
60
40
20
0
****
**
%TNF-α+
50
40
30
20
10
0
***
*
%IL-2+
50
40
30
20
10
0
**
D
Isotype
Anti-CD27
Anti-PD-1/L1
Combination
No. of cytokines
0
1
2
3

Figure 2

A

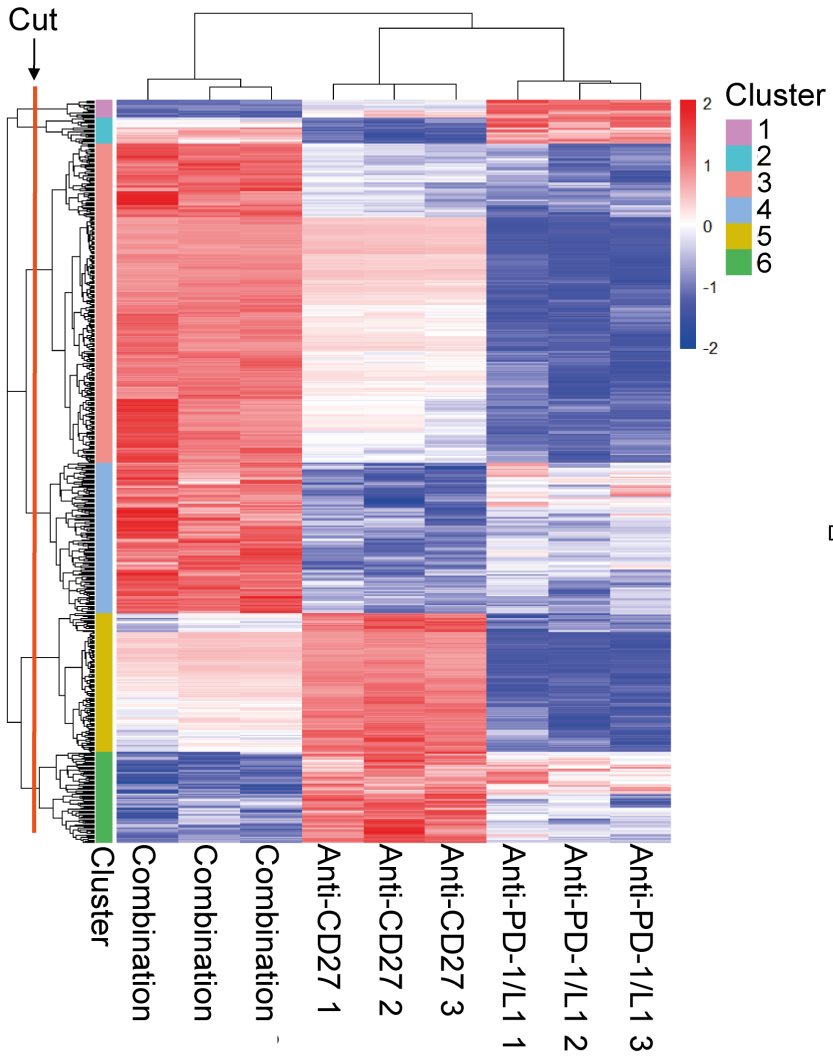

B

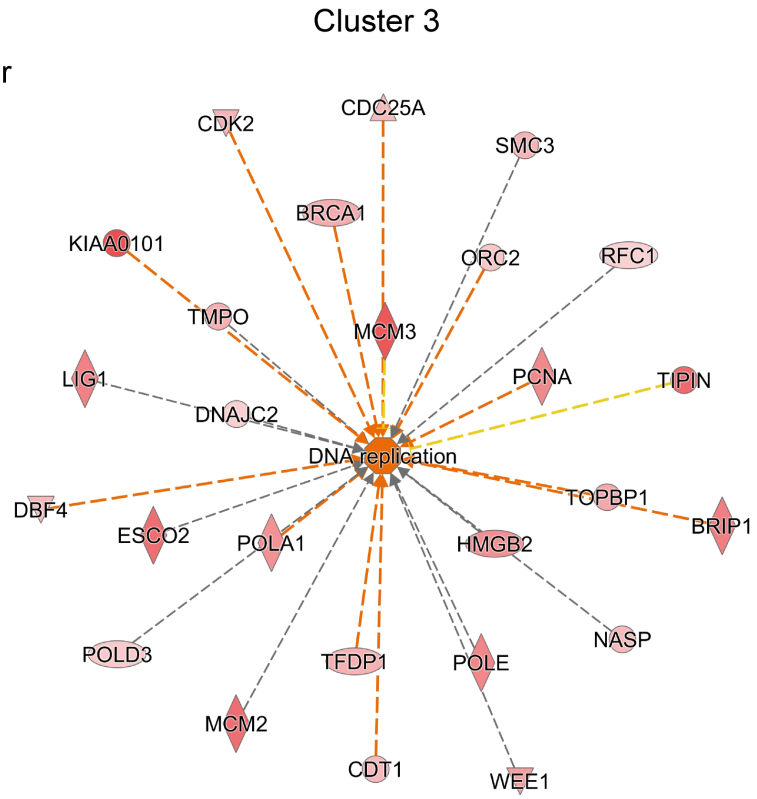

Process	*p value*	*z-score*
DNA replication	1.99×10^{-15}	2.741
Interphase	7.18×10^{-15}	2.405

C

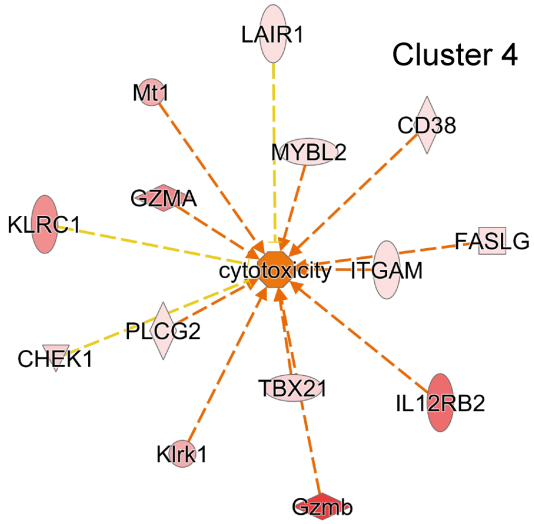

Process	*p value*	*z-score*
Cytotoxicity	1.44×10^{-10}	1.764
Proliferation of cells	4.66×10^{-10}	3.101

D

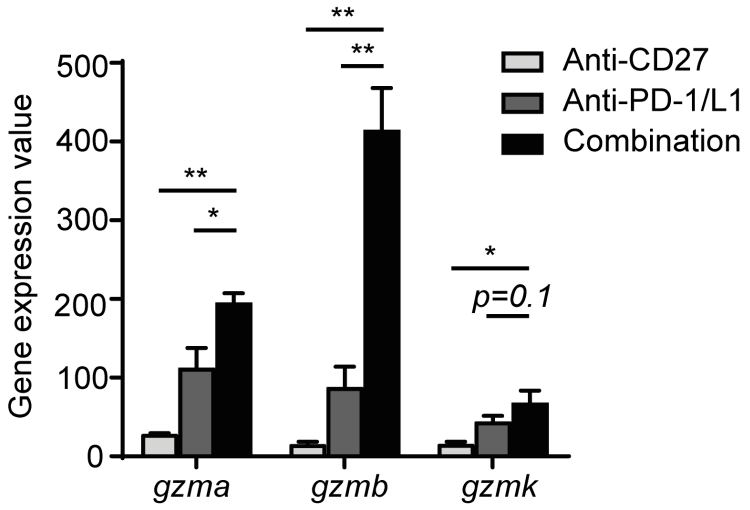

Figure 3

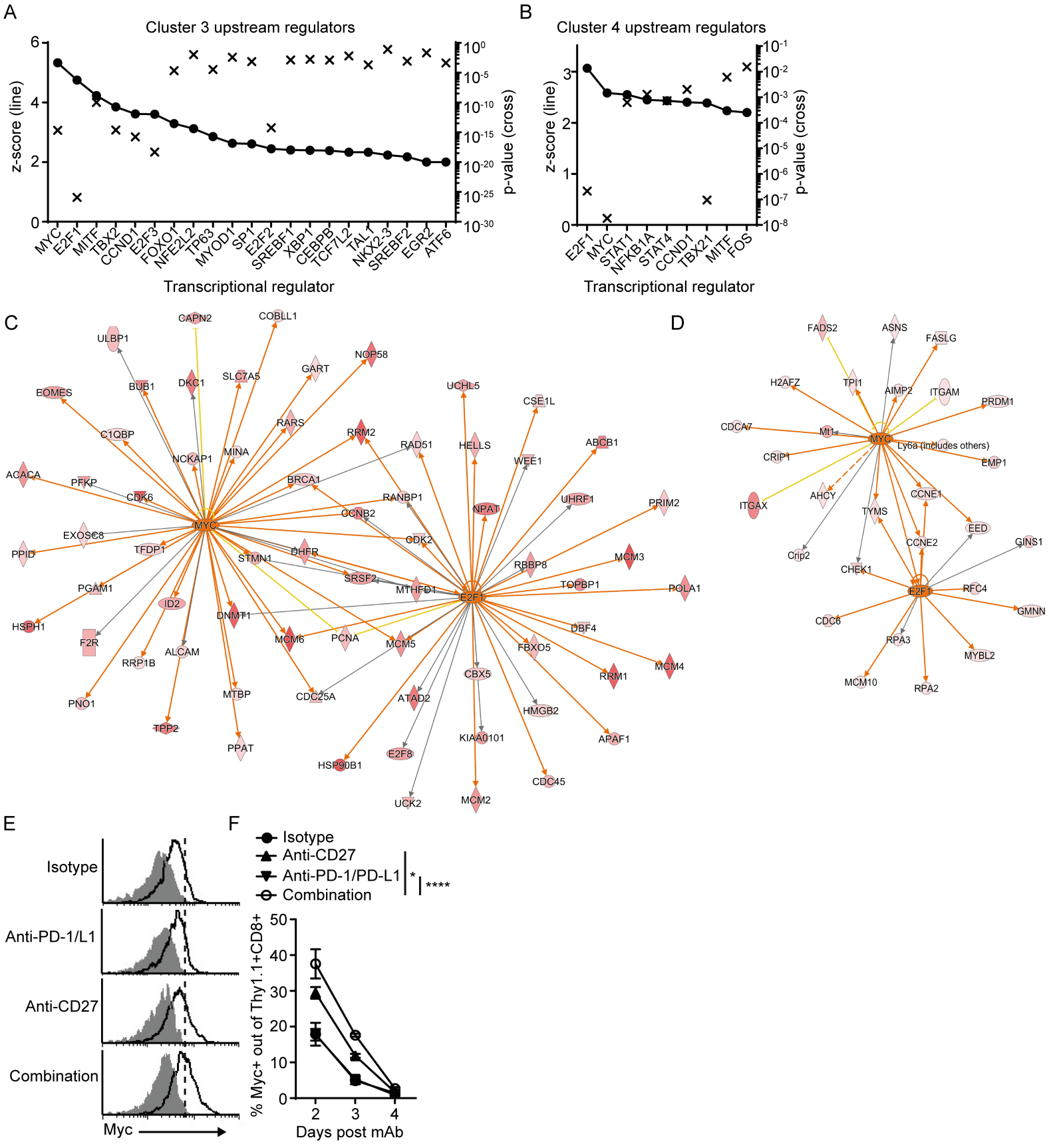
A
Cluster 3 upstream regulators
z-score (line)
p-value (cross)
MYC E2F1 MITF TBX2 CCND1 E2F3 FOXO1 NFE2L2 TP63 MYOD1 SP1 E2F2 SREBF1 XBP1 CEBPB TCF7L2 TAL1 NKX2-3 SREBF2 EGR2 ATF6
Transcriptional regulator
B
Cluster 4 upstream regulators
z-score (line)
p-value (cross)
E2F1 MYC STAT1 NFKB1A STAT4 CCND1 TBX21 MITF FOS
Transcriptional regulator
C
GAPN2 COBLL1 ULBP1 NOP58 GART SLC7A5 DKC1 BUB1 EOMES UCHL5 CSE1L RARS RRM2 RAD51 HELLS ABCB1 C1QBP NCKAP1 MINA WEE1 ACACA PFKP CDK6 BRCA1 RANBP1 UHRF1 PRIM2 NPAT CCNB2 MYC EXOSC8 CDK2 PPID TFDP1 STMN1 DHFR MCM3 RBBP8 SRSF2 TOPBP1 POLA1 PGAM1 MTHFD1 E2F1 ID2 DNMT1 DBF4 HSPH1 F2R MCM6 PCNA MCM5 FBXO5 MCM4 RRP1B ALCAM CBX5 RRM1 MTBP CDC25A ATAD2 HMGB2 PNO1 TPP2 KIAA0101 APAF1 PPAT E2F8 HSP90B1 CDC45 UCK2 MCM2
D
FADS2 ASNS FASLG H2AFZ TPI1 AIMP2 ITGAM PRDM1 CDCA7 Mt1 MYC Ly6a (includes others) CRIP1 EMP1 ITGAX AHCY CCNE1 TYMS EED CCNE2 GINS1 Crip2 CHEK1 E2F1 RFC4 GMNN CDC6 RPA3 MYBL2 MCM10 RPA2
E
Isotype
Anti-PD-1/L1
Anti-CD27
Combination
Myc
F
Isotype
Anti-CD27
Anti-PD-1/PD-L1
Combination
*
****
% Myc+ out of Thy1.1+CD8+
Days post mAb

Figure 4

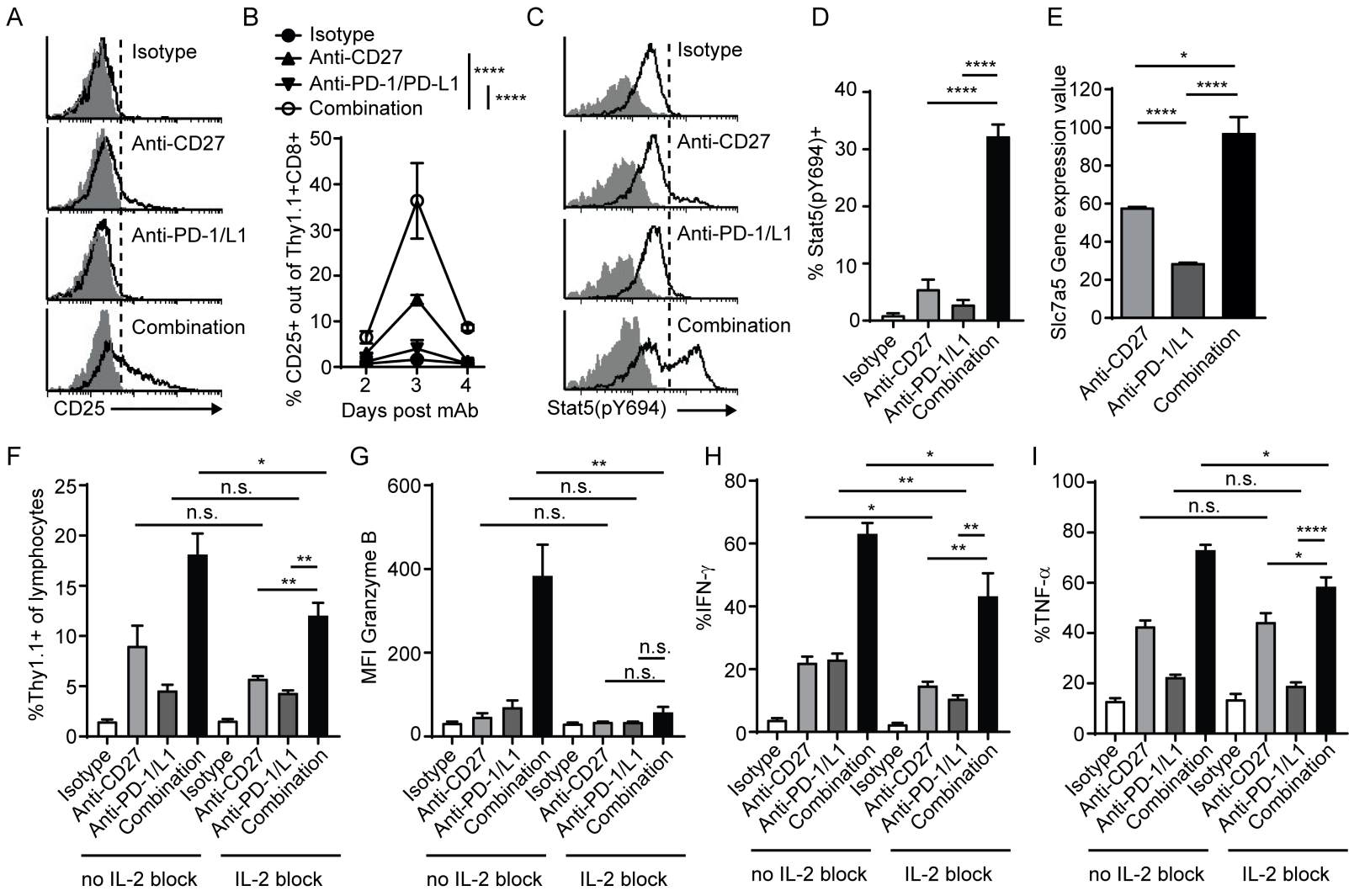
A
Isotype
Anti-CD27
Anti-PD-1/L1
Combination
CD25
B
Isotype
Anti-CD27
Anti-PD-1/PD-L1
Combination
****
****
% CD25+ out of Thy1.1+CD8+
Days post mAb
C
Isotype
Anti-CD27
Anti-PD-1/L1
Combination
Stat5(pY694)
D
% Stat5(pY694)+
****
****
Isotype
Anti-CD27
Anti-PD-1/L1
Combination
E
Slc7a5 Gene expression value
*
****
****
Anti-CD27
Anti-PD-1/L1
Combination
F
%Thy1.1+ of lymphocytes
*
n.s.
n.s.
**
**
Isotype
Anti-CD27
Anti-PD-1/L1
Combination
no IL-2 block
IL-2 block
G
MFI Granzyme B
**
n.s.
n.s.
n.s.
n.s.
H
%IFN-γ
*
**
*
**
**
I
%TNF-α
*
n.s.
n.s.
****
*

Figure 5

A

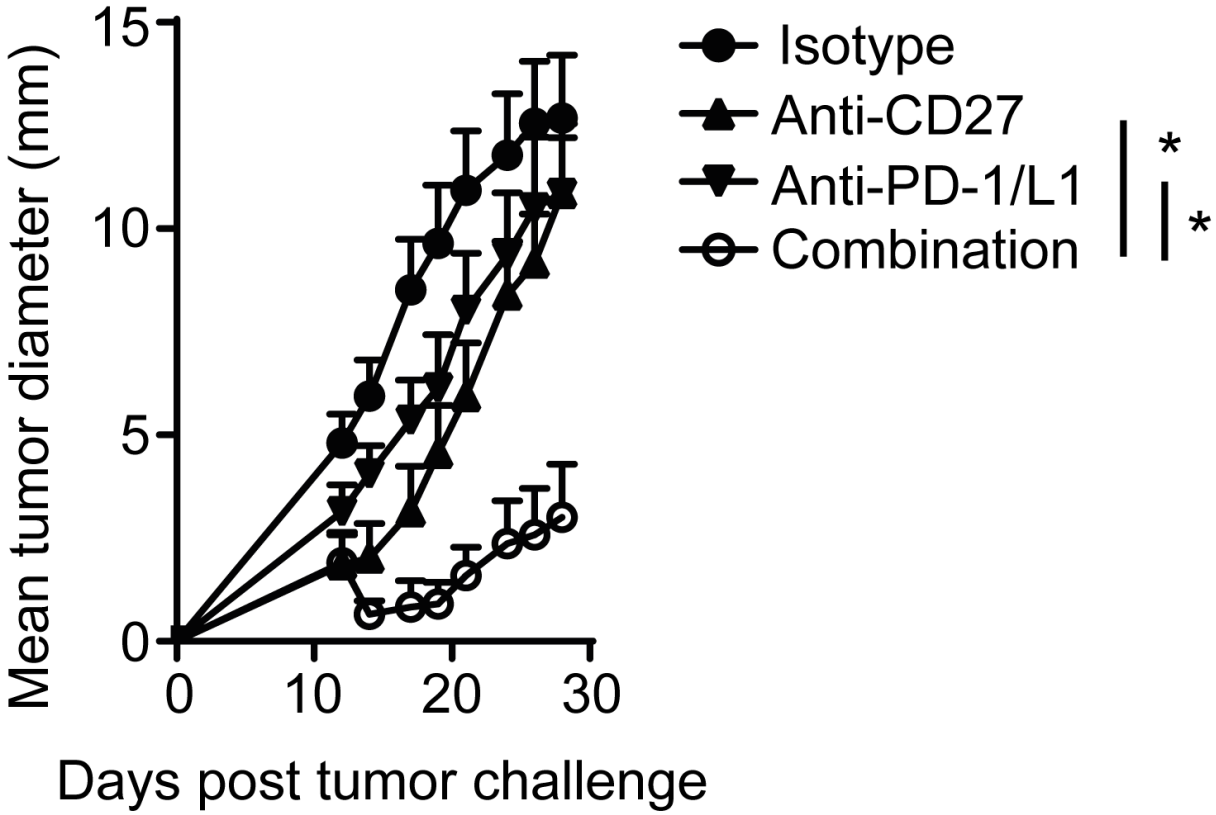
Mean tumor diameter (mm)
15
10
5
0
0
10
20
30
Days post tumor challenge
Isotype
Anti-CD27
Anti-PD-1/L1
Combination
*
*

B

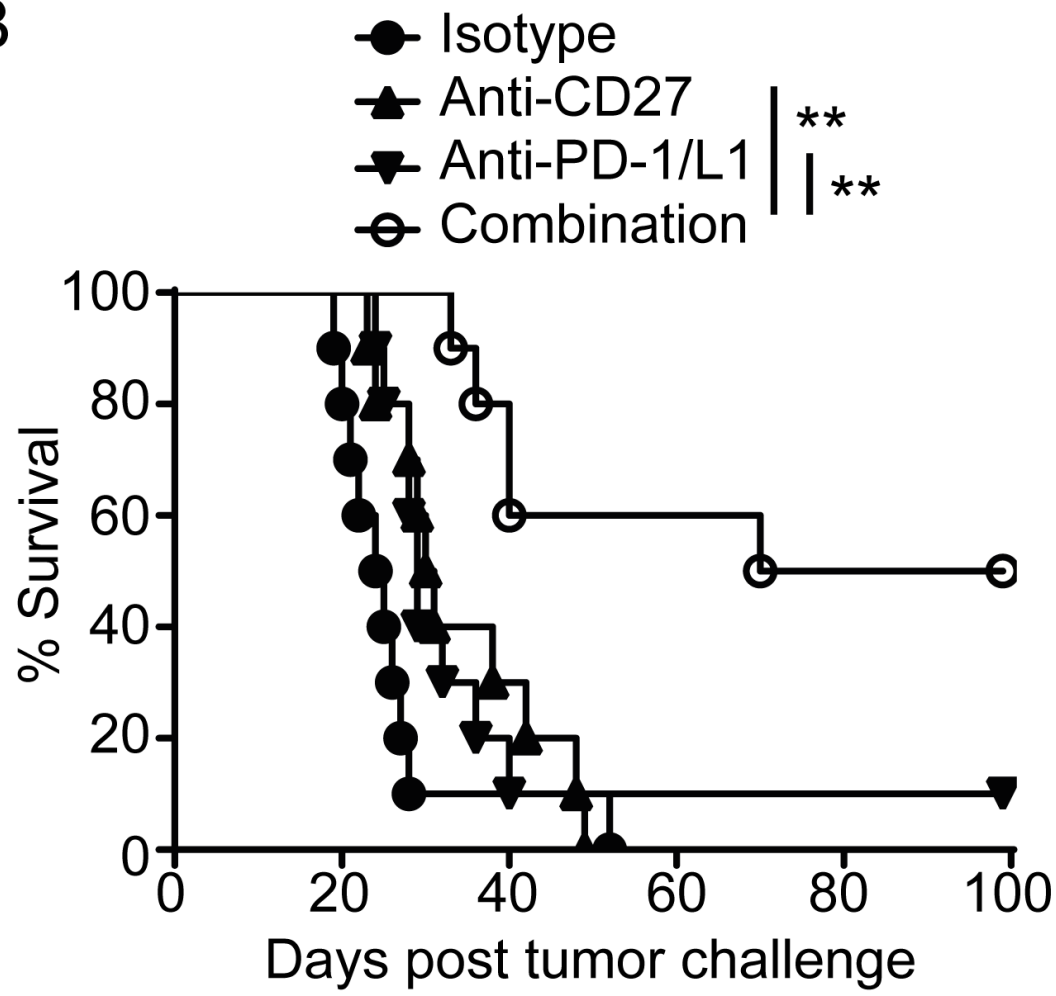
Isotype
Anti-CD27
Anti-PD-1/L1
Combination
**
**
% Survival
100
80
60
40
20
0
0
20
40
60
80
100
Days post tumor challenge

Figure 6

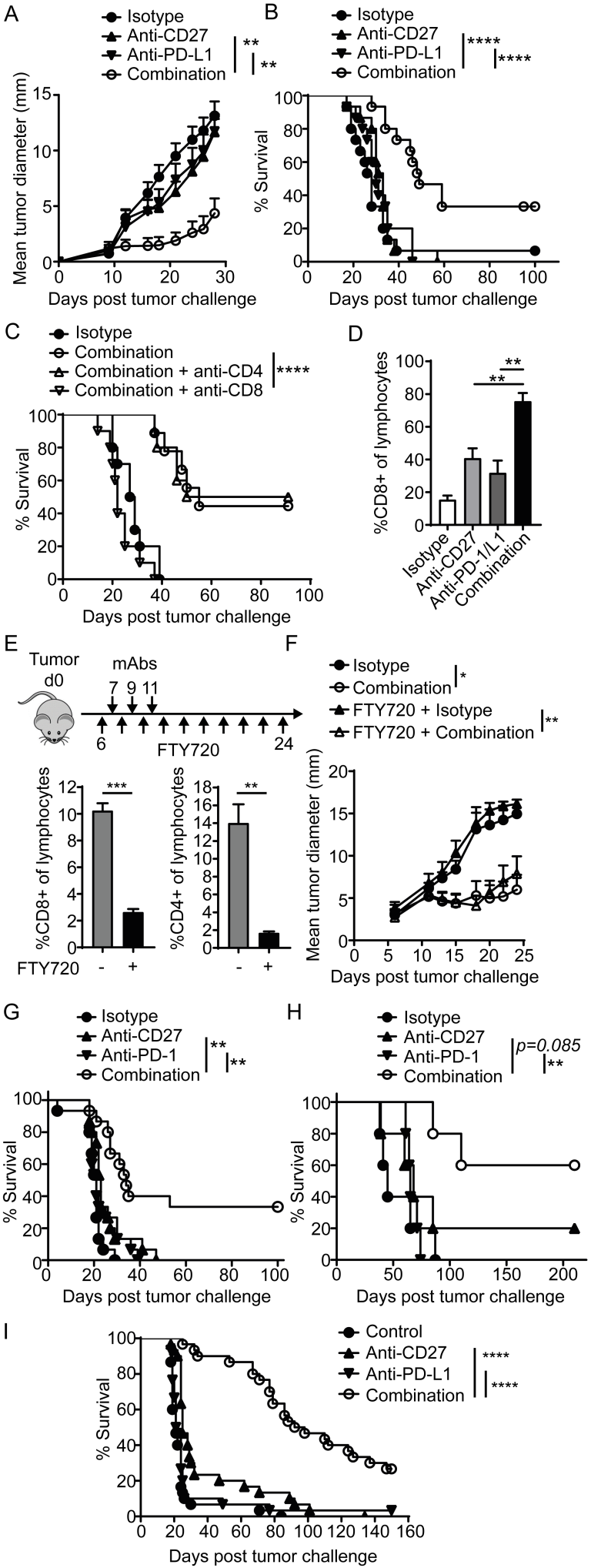
A
Isotype
Anti-CD27
Anti-PD-L1
Combination
**
**
Mean tumor diameter (mm)
Days post tumor challenge
B
Isotype
Anti-CD27
Anti-PD-L1
Combination
****
****
% Survival
Days post tumor challenge
C
Isotype
Combination
Combination + anti-CD4
Combination + anti-CD8
****
% Survival
Days post tumor challenge
D
**
**
%CD8+ of lymphocytes
Isotype
Anti-CD27
Anti-PD-1/L1
Combination
E
Tumor
d0
mAbs
7 9 11
6
FTY720
24
***
%CD8+ of lymphocytes
**
%CD4+ of lymphocytes
FTY720 - +
- +
F
Isotype
Combination
*
FTY720 + Isotype
FTY720 + Combination
**
Mean tumor diameter (mm)
Days post tumor challenge
G
Isotype
Anti-CD27
Anti-PD-1
Combination
**
**
% Survival
Days post tumor challenge
H
Isotype
Anti-CD27
Anti-PD-1
Combination
p=0.085
**
% Survival
Days post tumor challenge
I
Control
Anti-CD27
Anti-PD-L1
Combination
****
****
% Survival
Days post tumor challenge